RSC Advances

ROYAL SOCIETY OF CHEMISTRY

www.rsc.org/advances

RSC advances

ARTICLE

Multi-components in-situ and in-step formation of response visible-light C-dots composite TiO_2 mesocrystals

Received 00th January 20xx,
Accepted 00th January 20xx

DOI: 10.1039/x0xx00000x

www.rsc.org/

Dong Yan,[a,b] Yun Liu,*[a] Chun-yan Liu,*[a] Zhi-ying Zhang,[a] Shi-dong Nie,[a]

Carbon dots (C-dots) modified mesocrystal TiO_2 photocatalysts have been synthesized by a solvothermal process with L-ascorbic acid (LA) as a carbon source. The novel photocatalyst exhibited considerably visible light absorption, larger specific surface area (>100 m^2/g) and abundant mesopore structures. Compared with P25 and the prepared single mesocrystal TiO_2, C-dots modified mesocrystal TiO_2 demonstrated robustly visible photoactivity for the degradation of methyl orange (MO). Based on the characterization and analysis, an in-situ and in-step formation mechanism for C-dots and mesostructured TiO_2 composites via the complexation of LA with Ti-precursors has been proposed. And the experimental results with other carbon precursors confirmed the supposition. This work contributed novelty high surface area and mesopore structured photocatalysts responding to visible light and provided a simple strategy for the preparation of C-dots-TiO_2 composite structures.

1 Introduction

Among all of the photocatalysts, titanium dioxide is the most deeply-studied for its wonderful characteristics like chemical durability, non-toxicity, easy access and good photoactivity. However, its wide bandgap has limited the photoactivity of pure phase titanium dioxide to ultraviolet region, which accounts for only 5% of the total solar energy. In the past decades, great attention has been paid to extending the photo-response of titanium dioxide to visible region. Therefore, many reformed preparation processes for TiO_2, such as doping with transitional metal ions or anionic, compositing with semiconductors with narrow bandgap, sensitizing with dyes et al, have been developed [1]. Of them, the modification with quantum dots (QDs) is a quite efficient way to develop the visible response of TiO_2. Prototypical quantum dots to sensitize TiO_2 are generally cadmium chalcogenides, like CdS, CdSe and CdTe et al [2-5]. However, these materials have serious drawbacks, including toxicity and leaching of cadimium ions, which boost us to seek for novel materials and more eco-friendly ways to acquire equivalent or even better efficiency. Considering the advantages of nontoxicity, chemical and photo-stability, as the most attractive carbon materials emerged in recent years, carbon quantum dots (C-dots) is a better choice [6-9].

Until now, several strategies have been developed to combine C-dots with titania [10, 11]. For example, Liu group synthesized C-dots-TiO_2 nanorod sphere. They prepared C-dots and TiO_2 nanorod sphere in advance and then hydrothermal treatment of their mixture [12]. Zhang et al. developed a multi-step processes to obtain C-dots/rutile TiO_2 nanorod array. The method included the preparation of TiO_2 array and the C-dots, the adsorption of C-dots on the surface of TiO_2 array followed by annealing at moderate temperature [13]. C-dots/P25 heterojunctions was produced by hydrothermal treatment of the mixture of P25 and pre-prepared C-dots [14]. Huang et al. reported the synthesis of N-doped C-dots/rutile TiO_2 hierarchical microspheres by the hydrothermal treatment of $TiCl_3$ in the presence of N-doped C-dots [15]. C-dots/TiO_2 nanosheet composites had been fabricated by the mixture of pre-prepared C-dots and TiO_2 nanosheet [16]. In brief, the methods introduced above generally involved in several processes, such as the pre-preparation of C-dots and TiO_2, the immobilization of C-dots on TiO_2. Undoubtedly, all these are very time-consuming, cumbersome and tedious, and unfavorable to large-scale preparation and applications. Recently, Wang et al synthesized C-dots/TiO_2 microcrystal composites by one-pot process [17]. However, the improvement in visible absorption of the product was very limited, possibly due to the low loading amount of C-dots and small surface area of TiO_2 substrates.

[a] Key Laboratory of Photochemical Conversion and Optoelectonic Materials, Technical Institute of Physics and Chemistry, Chinese Academy of Sciences, Beijing 100190, China.
[b] University of Chinese Academy of Sciences, Beijing 100049, China.
* Corresponding authors:
Chunyan Liu, Email: cyliu@mail.ipc.ac.cn
Yun Liu, Email: liuyun@mail.ipc.ac.cn

Generally, the performance of a composite TiO_2 photocatalyst was not only related to the features of sensitizers, but also deeply influenced by the structure of TiO_2 matrix [18, 19]. Definitely, to obtain good performances and applications in photocatalysis and photovoltaic devices, integrating high crystallinity and high porosity into one material is the best selection. As crystallographically oriented assemblies of nanocrystals, mesocrystals not only contain similar single-crystal-like atom structures and scattering behaviours to conventional single crystals but also have rich porous structure [20, 21]. Different from traditional mesoporous materials, mesocrystal materials have comprehensively good crystallinity and high porosity. With the help of the merits of mesocrystal materials, combining C-dots with mesocrytal TiO_2 ($mcTiO_2$) by a simple method is very important. However, up to today, this has been few reported.

In the present work, we focus our attention on C-dots composite mesocrystal titania photocatalysts (C-dots-$mcTiO_2$). Through a simple one-pot solvothermal process, we realized the in-situ and in-step preparation of $mcTiO_2$, C-dots and the graft of C-dots on TiO_2. The as-prepared C-dots-$mcTiO_2$ demonstrated higher visible photoactivity in the degradation of methyl orange than the commonly used P25, the prepared single $mcTiO_2$ and C-dots/P25 composite prepared through multi-step method. Based on the investigation, it was suggested that the complexation between carbon sources and titanium ions played a dominant role in the formation of C-dots-$mcTiO_2$ composite. In order to confirm the supposition, we used glucose, lysine and citric acid as carbon precursors to prepare C-dots-$mcTiO_2$ and a similarly perfect result was achieved in the case of glucose and lysine. The method reported here offers not only advantages over the existing strategies for facile and efficient process, but also a new thinking in design and synthesis of similar composite photocatalysts.

2 Experimental sections

2.1 Reagents

Tetrabutyl titanate (TBT), anhydrous ethanol, acetic acid, and methyl orange (MO) were all of analytical grade and purchased from Beijing Chemical Factory. Analytical grade L-ascorbic acid (LA) was from Aobo Biological Technology Co., Ltd.

2.2 Synthesis of C-dots-$mcTiO_2$ composite

Under stirring, a certain amount of LA, 5ml acetic acid, 5ml anhydrous ethanol and 4.6ml TBT were added into a beaker and then the mixture was transferred into a Teflon-lined stainless-steel autoclave followed by heating at 180°C for 18h. The obtained solid product was centrifuged, washed with ethanol for several times, collected by further centrifugation and dried at room temperature. To explore the effects of C-dots on the structure and property of the final products, different amounts of LA (0, 0.05g, 0.1g, 0.2g, 0.3g and 0.4g) were used to prepare C-dots-$mcTiO_2$ composites which were named as A, B, C, D, E, F, separately.

2.3 Photocatalytic activity measurement

The photocatalytic activities of the prepared catalysts were evaluated by the degradation of MO under visible light. The photocatalyst (1g/L) and MO ($4*10^{-5}$mol/L) were dispersed in 40ml deionized water and sonicated for 20min, and then the pH value of the suspension was adjusted to 3.0 with 0.1mol/L HCl aqueous solution. The mixture was transferred into a glass photoreactor and stirred in the dark for 1h. When the absorption-desorption equilibrium in the system reached, oxygen was bubbled slightly into the solution for another 30 minutes. After that the reaction was carried out under the illumination of a 300 W high pressure Xe lamp with a Pyrex glass tube and an appropriate cut-off filter to cut off light shorter than 400 nm. During the photocatalytic reaction, stirring and a stream of oxygen gas was maintained. About 4ml of the reaction solution was drawn from the system every 30 min and centrifuged to remove the photocatalyst, the supernatant was used for the UV-vis spectral measurement. The peak value of MO at around 500nm was used to indicate the concentration of MO residual.

2.4 Characterization

The morphology of the as-synthesized sample was measured by JEOL JEM-2100 transmission electron microscope (TEM). XRD patterns were recorded on a Bruker D8 focus X-ray diffractometer. The nitrogen adsorption-desorption isotherms were conducted at 77K on a Micrometritics ASAP2000 system. Thermogravimetric analysis was performed on a TA SDT-Q600 analyzer. The UV-vis absorption spectra of different samples were obtained by a Varian Cary 5000 UV-Vis-IR spectrophotometer. Fourier Transform Infrared spectra were recorded by a Varian Excalibur 3100 FT-IR Spectrometer. The absorption spectra of MO aqueous liquid were monitored by a Shimadzu UV-1601 spectrophotometer. X-ray photoelectron spectroscopic (XPS) measurements were performed on a Thermo Electron Corporation ESCALAB 250 XPS spectrometer using a monochromatized Al Kα radiation (1486.6 eV).

3 Results and discussion

Table 1 Effect of LA on the crystalline size of C-dots-mcTiO_2: (a) The amount of LA used, (b) crystalline size of TiO_2 calculated by Debye-Scherrer equation

sample	A	B	C	D	E	F
[(a)]LA(g)	0	0.05	0.1	0.2	0.3	0.4
[(b)]D(nm)	12.0	11.3	11.0	10.6	7.8	8.0

XRD patterns of the prepared mcTiO_2 (sample A) and C-dots-mcTiO_2 (sample B-F) in Fig 1 indexed to the pure anatase phase (JCPDS Card No. 21-1272). Comparatively, the intensity of diffraction peaks decreased gradually with the increase of LA added, suggesting the decrease of crystallinity and crystalline size of the composite TiO_2 (Table 1). Additionally, there was no obvious peaks shift or other peaks in the XRD patterns, indicating the formed carbon with amorphous nature and not into the crystal of TiO_2.

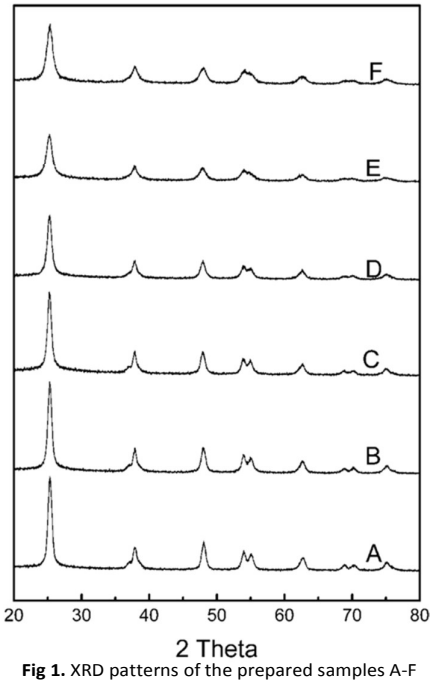

Fig 1. XRD patterns of the prepared samples A-F

As TEM images exhibited in Fig 2, the samples A, B and C showed granular morphologies with good crystallinity and abundant pore structures and clear lattice fringes of ca.0.35nm corresponding to the spacing of (101) planes of anatase in the insets. The average particle sizes based on TEM were 12.8nm, 10.6nm and 12.0nm for the sample A, B and C respectively, close to the size calculated by Debye Scherrer equation (Table 1), indicating that nanoparticles observed in the TEM images were single crystals, which confirmed mesocrystal structures of the sample A, B and C. However, when the LA amount was more than 0.2g or larger (the samples D-F), the corresponding TEM images exhibited more diversity and nanoparticles agglomeration became more serious. And with the increase of LA, more black small spots appeared on the nanoparticles, suggested the existence and content increase of C-dots. Since no lattice fringes of graphite were detected on these spots, we claimed that the C-dots were of amorphous nature, in line with that of XRD results.

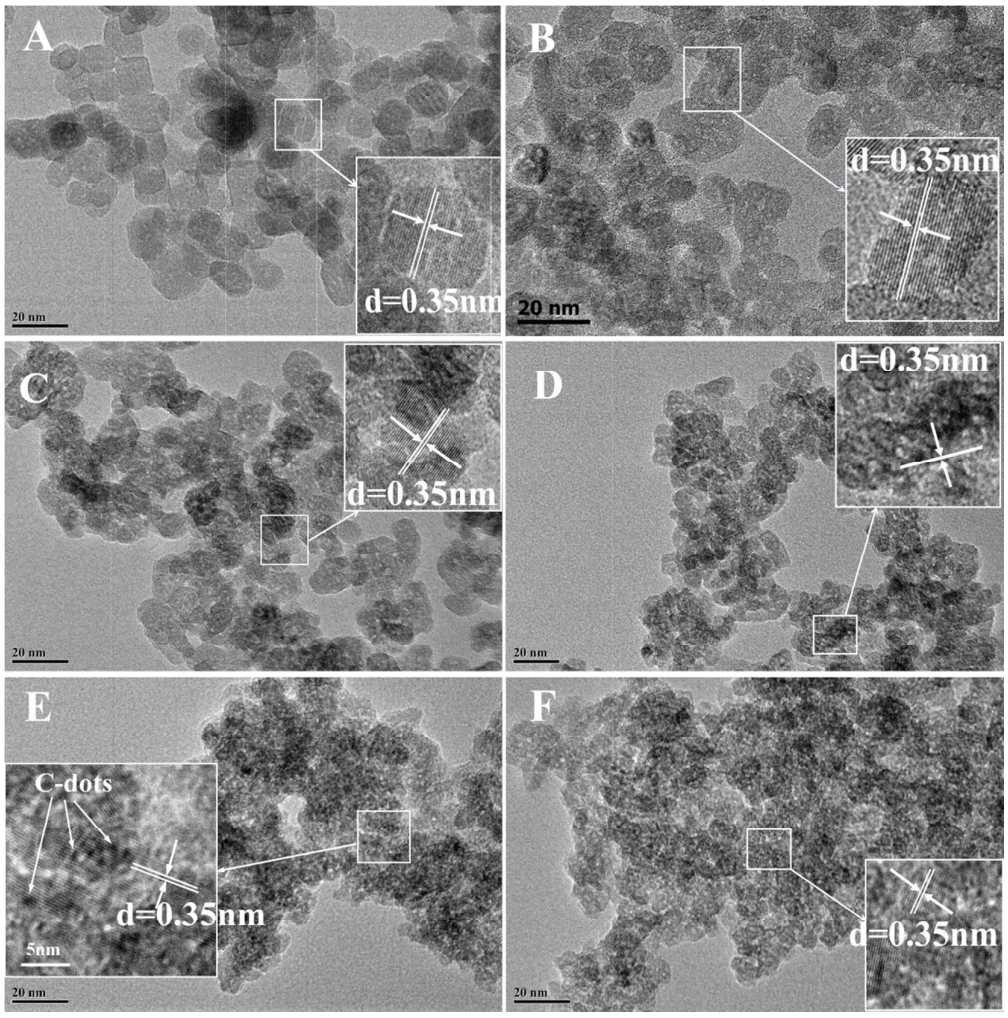

Fig 2. TEM images of the prepared samples A-F, inserts are the TEM view of the marked area with larger maginification

The nitrogen adsorption-desorption method was used to estimate the pore structure and surface area of photocatalysts. As shown in Fig 3, the adsorption-desorption isotherms can be classified into type IV according to BDDT with obvious hysteresis loop at higher relative pressure, indicating the presence of mesoporous structure[22]. The pore size distribution calculated by the BJH method revealed obvious difference in their pore structure. The sample A, B and C had a bimodal pore size distribution. One is in 1.4-2.4nm (the arrow marked region in Fig.3b), possibly from the pore in particle, and the other is larger (4.3-16.4nm), derived from the aggregation of particles. In the samples D, E and F, only large pore (6.0-11.2nm) was

observed, which should be related to the aggregation of particles, where small pore disappeared due to the block of C-dots to the pores within particle. With continuously increasing C-dots, particles aggregated more badly while surface roughness increased induced by C-dots covering, leading to a decrease in pore diameter of the sample.

The specific surface area (S_A) and pore volume of the six samples were listed in Table 2. It was found that the S_A of six samples was all larger than 100m^2/g and increased gradually from A to F, mainly due to the increase of surface roughness of the C-dots-mcTiO_2 by the covering of C-dots. It is worth mentioning that the S_A of the sample E and F even reached 160m^2/g, far more than 88m^2/g ever reported[11]. Large S_A generally benefits to the adsorption of reactive species and accordingly favors good photocatalytic activity. Different from S_A, the pore volume increased first from the sample A to D, reached a maximum and then declined.

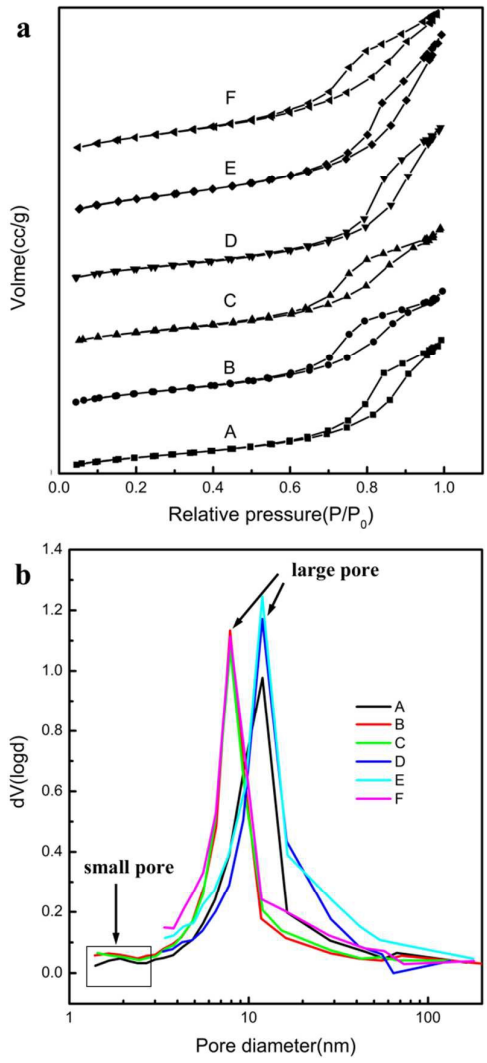

Fig 3. Adsorption-desorption isotherms (a) and pore size distribution curves of the samples A to F (b)

Table 2. The pore structure of C-dots-mcTiO_2 composites: specific surface area (S_A) and pore volume of the samples A-F based on BET analysis results

Sample	LA (g)	S_A (m^2/g)	Pore volume (cc/g)
A	0	102.7	0.36
B	0.05	116.2	0.33
C	0.1	111.9	0.41
D	0.2	118.8	0.47
E	0.3	165.0	0.49
F	0.4	164.4	0.38

Definitely, the results in Fig 1-3 confirmed the structure, composition, pore volume and size of the as-prepared mesocrystal C-dots-mcTiO_2 composites. FTIR measurement further explained the action of C-dots in the composites. In Fig 4a, the broad absorption from 3200 cm^{-1} to 3500 cm^{-1} was attributed to the –OH vibration of H_2O adsorbed on TiO_2 and -OH directly on TiO_2, as well as –OH and –COOH functional groups on C-dots. The sharp absorption at around 2300 cm^{-1} was due to the vibration of CO_2 adsorbed on the surface. The general whole spectrum from 400-1000cm^{-1} depicted the main features of anatase TiO_2 [23]. Compared with the sample A, samples C-E showed a few sharp peaks located in the range of 1600 cm^{-1} and 1400 cm^{-1} (enlarged spectra in Fig 4b), attributed to C=C bond vibration in aromatic ring, which is one of the typical features of C-dots [24, 25]. The relative intensity of these feature peaks rose gradually from C to E, indicating the increasing amount of C-dots in the system. And a faint peak newly appeared at 1647cm^{-1} in the enlarged spectra of the samples C-E in Fig 4b was attributed to the stretching vibration of C=O bond connected to aromatic rings [26]. Obviously, C-dots have rich oxygen-containing groups, which benefit to the connection with TiO_2.

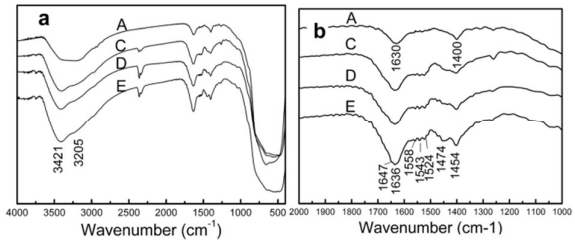

Fig 4. FT-IR spectrums of the prepared mcTiO_2 (sample A) compared with C-dots-mcTiO_2 composites (sample C, D and E)

To further study the interaction of C-dots with mcTiO_2 and chemical species in the products, XPS of the sample D (C-dots-mcTiO_2) and the sample A (mcTiO_2) were performed. The full-scale XPS spectrum of the sample D illustrated the existence of Ti, O and C (Fig. 5a). High resolution spectrum of C_{1s} could be separated into three bands at 284.7, 285.8 and 288.5eV corresponding to C=C, C-O and C=O, respectively[27], confirming the presence of C-dots. The peaks at 529.8 eV, 530.6 eV and 531.9 eV were used to fit the high resolution spectrum of O_{1s}

(Fig. 5b) and attributed to Ti-O, C-O and O-H bonds, respectively, further revealing the abundant oxygen-containing groups on C-dots in the composited system[28]. Compared with the sample A, the binding energy of Ti($2p_{1/2}$, 464.5 and Ti($2p_{3/2}$, 458.7 eV) of the sample D slightly shifted towards a higher binding energy (Fig. 5d), suggesting the strong interaction between TiO_2 and C-dots. Since no Ti-C peaks was observed in C1s, the interaction of C-dots and TiO_2 should be achieved through Ti–O–C bond[29, 30].

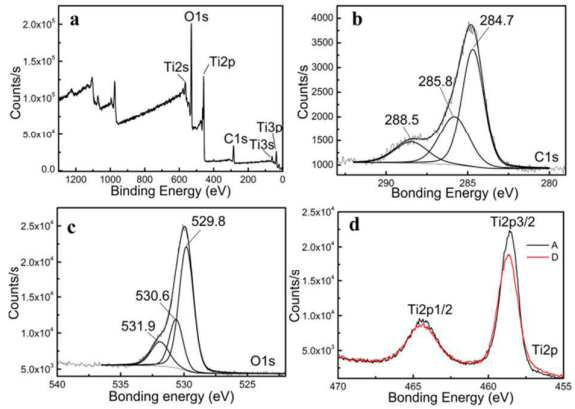

Fig 5. XPS analysis of the sample D: the full-scale XPS spectrum (a); high resolution XPS spectra of C 1s (b), O1s (c), and Ti 2p (d). The curve A (black) and D (red) in (d) were the high resolution Ti 2p XPS spectra of the sample A and D respectively

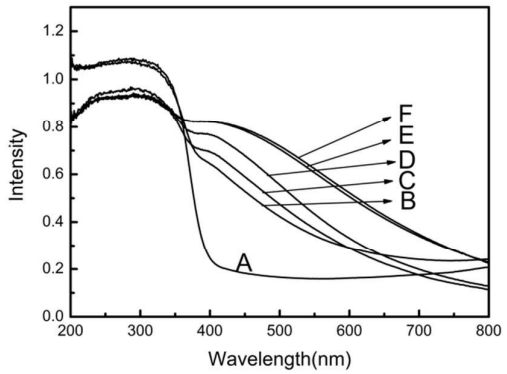

Fig 6. UV-Vis absorption spectra of the prepared $mcTiO_2$ (the sample A) and C-dots-$mcTiO_2$ (the samples B-F)

As depicted in Fig 6, the prepared single $mcTiO_2$ had little absorption in visible light region whereas visible absorption of the C-dots-$mcTiO_2$ improved evidently. With the increase of LA (C amount), the absorption intensity of the composite gradually enhanced, especially in longer wavelength. But the absorption for the sample E and F was almost the same, even though LA increased from 0.3 to 0.4 g. It is clear that the surface area of the prepared TiO_2 is certain, if the balance of C-dots and the surface area of TiO_2 reached, with the increase of LA amount, excess C-dots would stay in solvent instead of on TiO_2.

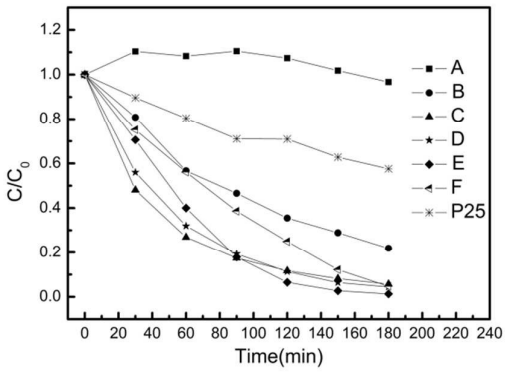

Fig 7. Photocatalytic properties of different samples: the prepared $mcTiO_2$ (sample A), C-dots-$mcTiO_2$ (the sample B-F) and P25

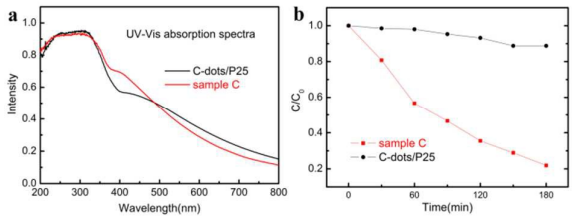

Fig 8. The comparison of the optical properties of C-dots-$mcTiO_2$ and P25/CDs: UV-Vis absorption spectra (a) and photocatalytic properties (b) of sample C and p25/CDs

As can be seen in Fig 7, the prepared single $mcTiO_2$ and commercial photocatalyst P25 had little visible light activity and C-dots modified samples showed booming visible response in the same condition. The initial photocatalytic rates over C-dots-$mcTiO_2$ enhanced from the sample B to C and D, and then decreased (E and F). The visible light absorption increased monotonically from the sample A to E (Fig.6), whereas the pore volume achieved the maximum in the samples C-D (Table 2). Clearly, besides light absorption, pore structures also played a significant role in the improvement of photocatalytic activity of C-dots-$mcTiO_2$.

The optical properties of C-dots-$mcTiO_2$ (the sample C) and C-dots composited P25 (C-dots/P25, prepared with the same LA concentration as the sample C, see Supporting information) were comparatively studied. As shown in Fig 8a, C-dots/P25 showed obviously weaker absorption in the region from 400nm to 550nm. Moreover, the photocatalytic activity of C-dots/P25 was much inferior to that of the sample C (Fig 8b). All these further confirmed the advantages of C-dots-$mcTiO_2$ composites developed in the present work. Because a larger specific surface area of the C-dots-$mcTiO_2$ (111.9m^2/g) made the possibly high loading amount of C-dots and thus led to better absorption in visible region; and the in-situ and in-step hydrothermal synthesis process made the bonding of C-dots and TiO_2 more effective and resulted in better optical and catalytic activities.

To clarify the formation mechanism of C-dots-mcTiO_2 through one-pot solvothermal process, we investigated the effect of LA. When LA was added into the mixture solution of TBT and acetic acid, the color of the solution turned from pale yellow to claret immediately, indicating the formation of Ti-chelate, which was further confirmed by the variation in their FT-IR spectra in Fig 9. As shown in the insert of Fig 9, there are three kinds of oxygen in LA. One is the oxygen of carbonyl, second is the oxygen of enol and the third is the oxygen of hydroxyl. The bands at 1755cm^{-1} and 1670 cm^{-1} should be attributed to the vibration of carbonyl and enol [31]. Upon the interaction of TBT with LA, the strong bands at 1755 cm^{-1} and 1670 cm^{-1} shifted to 1734 cm^{-1} and 1620 cm^{-1}, respectively, suggesting the coordination between LA and Ti^{4+} [32, 33].

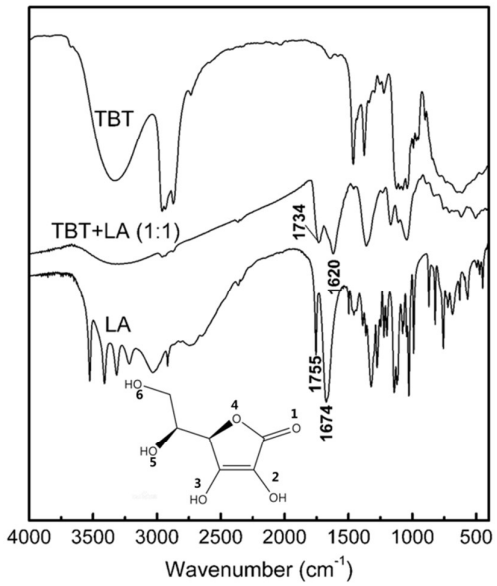

Fig 9. FT-IR spectra of pure TBT, TBT+LA (1:1 mol ratio) and free LA, inset is the molecular structure of LA

As mentioned above, the complexation between carbon source and TBT played a key role in the in-situ and in-step formation of C-dots in the TiO_2. To confirm the proposal, we employed glucose, lysine and citric acid as a carbon source and kept the other procedure the same to prepare C-dots-mcTiO_2. When glucose or lysine was added into the mixture of acetic acid, TBT and ethanol, the solution color turned from pale yellow to dark brown or red brown, whereas citric acid induced little change in the color. Depending on the color variation induced by the reaction of LA with TBT, it is reasonable to deduce that similar complexion took place in the presence of glucose or lysine. As expected, the prepared C-dots-mcTiO_2 used glucose or lysine demonstrated better visible absorption and photocatalytic activity than that from citric acid (Fig 10), and further confirmed the essential role of the complexation of carbon source and TBT for the formation of good C-dots composite TiO_2 photocatalyst.

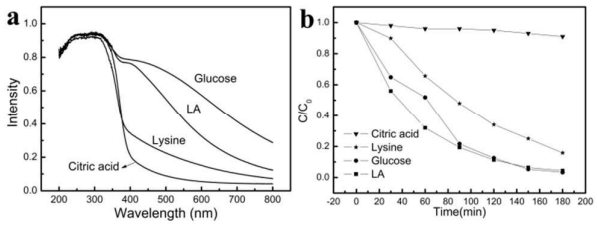

Fig 10. UV-Vis absorption spectra (a) and photocatalytic properties (b) of the different samples prepared with citric acid, lysine, glucose and LA as carbon sources

Based on the analysis above, a possible formation mechanism of the C-dots-mcTiO_2 is schematically explained in Fig 11. Three reactions possibly occurred in the autoclaves including acidolysis of Ti-precursor, exterification of ethanol with acetic acid [34] and the carbonization of carbon source to C-dots. Through acidolysis process, nascent nanocrystal TiO_2 with abundant hydrophobic groups formed and with the help of esters, nanocystals went through crystallographical self-assembly and crystallization processes, mcTiO_2 was obtained.

When LA was introduced into the reaction system, titanium ions chelated with LA. Due to the relative stability of Ti-LA coordinative structure, LA could be partly maintained on the surface of nascent nanospecies TiO_2 and even mcTiO_2. With the increase of the reaction time, the Ti-LA and LA on TiO_2 carbonized and aggregated then formed newborn C-dots anchored on the surface of nascent TiO_2 nanocrystals. Meanwhile the LA from the liquid phase carbonized and aggregated around anchored LA or newborn C-dots, thus C-dots formed right on the surface of TiO_2. Additionally, due to the effective interaction of LA and titanium ions, the crystal growing process was hindered [35, 36] and led to relatively smaller crystal sizes (Table 1). With excess LA, more C-dots formed at the same time. Moreover, newborn C-dots-mcTiO_2 composite single crystals easily linked via oxygen-containing groups on C-dots, leading to the serious agglomeration of particles (E and F) as illustrated in Fig 2.

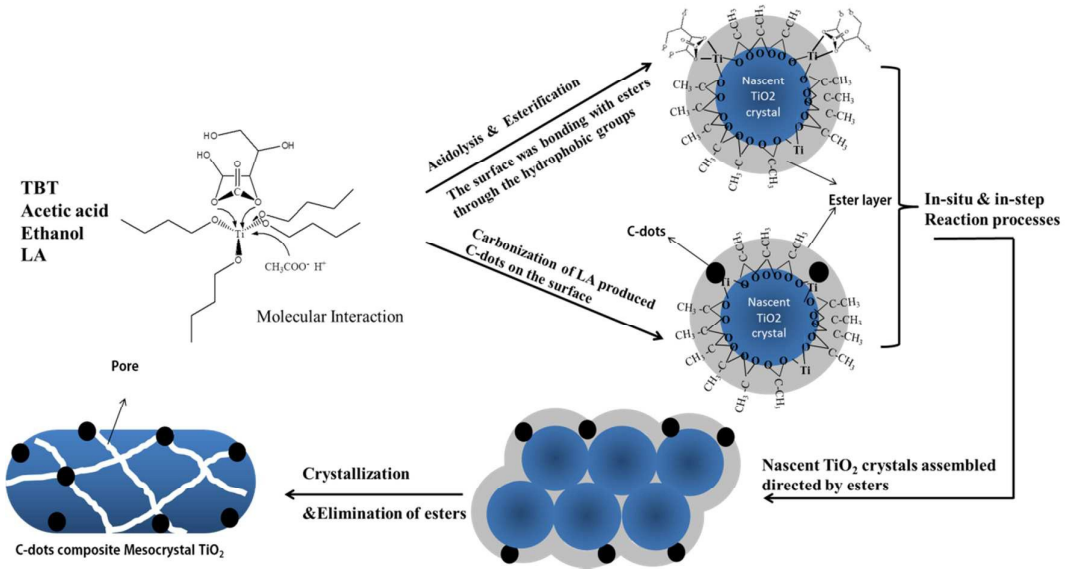

Fig 11. Illustration of formation mechanism of C-dots-mcTiO_2

Conclusions

In this work, C-dots composite TiO_2 mesocrystals were synthesized through a simple one-pot solvothermal method. It was certificated that light absorption of the TiO_2 has been effectively expanded to visible light region by the composite of C-dots and the final products demonstrated great visible light activity in the degradation of MO. An in-situ and in-step formation mechanism for C-dots and mesostructured TiO_2 microcrystals was proposed. During the synthesis, the complexation of carbon source and TBT (or other Ti precursors) was dominant to the in-situ and in-step formation of C-dots on TiO_2. In this work, we not only improved the photocatalytic activity of TiO_2 using C-dots as a sensitizer through an eco-friendly way, but also developed a new way to synthesize similar C-dots composites and offer a useful guide in the choice of carbon source towards effective synthesis.

Acknowledgements

The authors thank the support of National Natural Science Foundation of China (21103209 and 21273256).

References

1. L. X. Sang, Y. X. Zhao and C. Burda, *Chem. Rev.*, 2014, **114**, 9283-9318.
2. X. X. Yao, T. Y. Liu, X. H. Liu and L. D. Lu, *Chem. Eng. J.*, 2014, **255**, 28-39.
3. E. C. Hao, B. Yang, J.H Zhang, X. Zhang, J. Q. Sun, J. C. Shen, *J. Mater. Chem.*, 1998, **8**, 1327–1328.
4. X. G. Peng, M.C. Schalamp, A. V. Kadavanich, and A. P. Alivisatos, *J. Am. Chem. Soc.*, 1997, **119**, 7019-7029.
5. H. Gerischer and M. Lobke, *J. Electromul. Chem.*, (1986), 225-227.
6. S. N. Baker and G. A. Baker, *Angew. Chem. Int. Ed.*, 2010, **49**, 6726-6744.
7. H. Li, Z. Kang, Y. Liu and S.-T. Lee, *J. Mater. Chem.*, 2012, **22**, 24230.
8. A. B. Bourlinos, A. Stassinopoulos, D. Anglos, R. Zboril, V. Georgakilas and E. P. Giannelis, *Chem. Mater.*, 2008, **20**, 4539–4541.
9. F. Wang, S. Pang, L. Wang, Q. Li, M. Kreiter and C.-y. Liu, *Chem. Mater.*, 2010, **22**, 4528-4530.
10. H. Ming, Z. Ma, Y. Liu, K. Pan, H. Yu, F. Wang and Z. Kang, *Dalton Trans.*, 2012, **41**, 9526.
11. D. K. Chan, P. L. Cheung and J. C. Yu, *Beilstein J Nanotechnol*, 2014, **5**, 689-695.
12. J. Liu, W. Zhu, S. Yu and X. Yan, Carbon, 2014, **79**, 369-379.
13. J. Bian, C. Huang, L. Wang, T. Hung, W. A. Daoud and R. Zhang, *ACS Appl. Mater. Interfaces*, 2014, **6**, 4883-4890.
14. H. Yu, Y. Zhao, C. Zhou, L. Shang, Y. Peng, Y. Cao, L.-Z. Wu, C.-H. Tung and T. Zhang, *J. Mater. Chem. A*, 2014, **2**, 3344.
15. Y.-Q. Zhang, D.-K. Ma, Y.-G. Zhang, W. Chen and S.-M. Huang, *Nano Energy*, 2013, **2**, 545-552.
16. X. Yu, J. Liu, Y. Yu, S. Zuo and B. Li, *Carbon*, 2014, **68**, 718-724.
17. W. Wang, Y. Ni and Z. Xu, J. Alloys Compd., 2015, **622**, 303-308.
18. K. Bourikas, C. Kordulis and A. Lycourghiotis, *Chem. Rev.*, 2014, **114**, 9754-9823.
19. L. Liu and X. Chen, *Chem. Rev.*, 2014, **114**, 9890-9918.
20. H. Colfen and M. Antonietti, *Angew. Chem. Int. Ed. Engl.*, 2005, **44**, 5576-5591.
21. L. Zhou and P. O. Brien, *Small*, 2008, **4**, 1566-1574.
22. K. S. W. Sing, D. H. Everett, R. A. W. Haul, L. Moscou, R. A. Piertti and T. S. J. Rouquerol, *Pure Appl. Chem.*, 1985, **57**, 603.
23. L. Ojamae, C. Aulin, H. Pedersen and P. O. Kall, *J. Colloid Interface Sci.*, 2006, **296**, 71-78.
24. R. Liu, D. Wu, X. Feng and K. Mullen, *J. Am. Chem. Soc.*, 2011, **133**, 15221-15223.
25. X. Yan and L.-S. Li, *J. Mater. Chem.*, 2011, **21**, 3295.

26. B. Zhang, C.-y. Liu and Y. Liu, *Eur. J. of Inorg. Chem.*, 2010, **2010**, 4411-4414.
27. H. Ago, T. Kugler, F. Cacialli, W. R. Salaneck, M. S. P. Shaffer, A. H. Windle, R. H. Friend, *J. Phys. Chem. B*, 1999, **103**, 8116-8121.
28. A. S. Lim, A. Atrens, *Appl. Phys. A*, 1990, **51**, 411-418.
29. Y. Cong, X. Li, Y. Qin, Z. Dong, G. Yuan, Z. Cui and X. Lai, *Appl. Catal. B: Environmental*, 2011, **107**, 128-134.
30. B. Liu, Y. Huang, Y. Wen, L. Du, W. Zeng, Y. Shi, F. Zhang, G. Zhu, X. Xu and Y. Wang, *J. Mater. Chem.*, 2012, **22**, 7484.
31. J. Hvoslef and P. Kleaboe, *Acta Chem.Scand.*, 1971, **25**, 3043-3053.
32. H. A. Tajmir-Riahi, *J. Inorg. Biochem.*, 1990, 181-188.
33. B. Zumreoglukaran, *Coord. Chem. Rev.*, 2006, 250, 2295-2307.
34. L. Li and C.-y. Liu, *CrystEngComm*, 2010, **12**, 2073.
35. Y. W. Jun, M. F. Casula, J.-H. Sim, S. Y. Kim, J. Cheon and A. P. Alivisatos, *J. Am. Chem. Soc.*, 2003, **125**, 15981-15895.
36. Y. Liu, C.-y. Liu and Z.-y. Zhang, *Chem. Eng. J.*, 2008, **138**, 596-601.

Graphical abstract:

Multi-components in-situ and in-step formation of response visible-light C-dots composite TiO_2 mesocrystals

By

Dong Yan, Yun Liu, Chun-Y Liu*, Zhi-Y Zhang, Shi-D Nie*

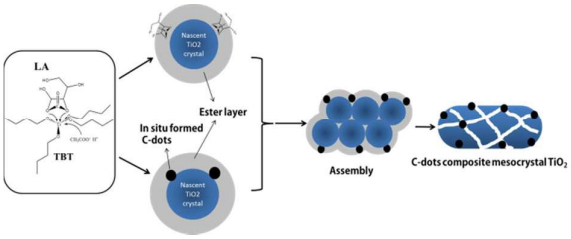

Successful in-situ and in-step formation of C-dots composited TiO_2 mesocrystals is closely related to the complexation between carbon source and Ti ion.